

A98-31577

NONLINEAR CHARACTERISTICS OF TRANSONIC FLUTTER OF A HIGH ASPECT RATIO WING

Hiroshi Matsushita*, Kenichi Saitoh†

* Director for Special Research

† Researcher, Advanced Aircraft Technology Project Center
National Aerospace Laboratory, Mitaka, Tokyo 181-0015, Japan

and

Péter Gránásy

Engineer, Productivity Center
GE Lighting Europe, 1340 Budapest, Hungary

Wind tunnel model of a high aspect ratio wing for active flutter control study enters flutter of limit cycle oscillation (LCO) type. In order to get better understanding and mathematically modeling the transonic flutter for active control, wind tunnel tests were conducted. During the tests, a typical nonlinear dynamics emerged; a nominal flutter without any intentional excitation occurred as a large amplitude limit cycle oscillation (LC- II) via a subcritical Hopf bifurcation in conjunction with saddle-node bifurcation, while a small amplitude limit cycle oscillation (LC- I) appeared as a supercritical Hopf bifurcation. In particular, LC- II occurred at well below the nominal flutter dynamic pressure if the wing was excited by a leading edge control surface. This limit cycle oscillation remained stable until almost 10% lower dynamic pressure than nominal value where LCO vanished via a saddle-node bifurcation. Quantitative bifurcation diagram was thus obtained by the test and an empirical math model of single degree-of-freedom is proposed. Furthermore, LC- I was realized by disengaging a flutter control at a slightly higher dynamic pressure than nominal value. As the dynamic pressure was further decreased, this LC- I disappeared in a supercritical Hopf-bifurcation. This paper analyzes these new findings obtained in the tests by the nonlinear dynamics framework.

Introduction

In transonic region flutter dynamic pressure drops significantly, particularly for a high aspect ratio wing, known as the transonic dip phenomena. Furthermore, transonic flutter often takes the form of limit cycle oscillation (LCO). The fact that flutter in transonic region often takes a limit cycle oscillation has long been recognized and we have excellent review monographs written by Cunningham⁽¹⁾ and by Dowell.⁽²⁾ LCO is caused by two nonlinearity, aerodynamics oriented and structures oriented. Even if confined in aerodynamics nonlinearity, many researchers have

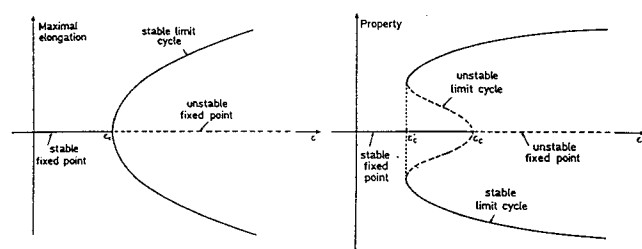
treated the topics including Ueda and Dowell,⁽³⁾ Bendiksen⁽⁴⁾ and others. Nakamichi succeeded in realizing LCO by CFD analysis using Navier-Stokes code⁽⁵⁾. Experimental observations of LCO have also reported by many researchers.⁽⁶⁻⁸⁾

Among these many research work, present research aims at getting more deep insight into the effect of dynamic pressure change on the characteristics change of LCO, i. e., bifurcation nature. There is few study experimentally realizes LCO and investigates the effect of excitation upon the bifurcation characteristics of LCO. In order to get better understanding of the limit cycle oscillation of the transonic flutter, intending to provide experimental data for validating the analytical expectation and to improve the mathematical model for active flutter control, wind tunnel tests were conducted. A wind tunnel model of a high aspect ratio aeroelastic wing for active flutter control study was entered flutter of LCO type in the transonic wind tunnel at National Aerospace Laboratory, Japan.

Nonlinear dynamics tell us two typical bifurcation. Most well known is supercritical Hopf bifurcation represented by van del Pol equation.^(9,10)

$$\ddot{x} - (\varepsilon - \varepsilon_c - x^2)\dot{x} + x = 0$$

Bifurcation diagram as the parameter ε varies takes the form as shown in Fig. 1(a).



(a) Supercritical

(b) Subcritical

Fig. 1 Hopf bifurcation

Another complementary one is subcritical Hopf bifurcation. Its equation is created from van der Pol equation by destabilizing second power term and introducing forth power term for stabilization, resulting as,

$$\ddot{x} - (\varepsilon - \varepsilon_c - x^2 - 0.5x^4)\dot{x} + x = 0$$

Bifurcation diagram corresponding to this equation is shown as in Fig.1(b). In practice, flutter of in a subcritical type should be more concerned since it is violent in nature. Limit cycle flutter treated here is well explained by these diagram particularly by the latter one.

This paper analyzes these several experimental findings by the nonlinear dynamics framework.

Basic Nonlinearity Observed in Transonic Wind Tunnel Tests

High Aspect Ratio Wing Model

A flutter model which was entered in the wind tunnel tests is shown in Fig. 2. It was refurbished from a high aspect ratio wing in order to implement a leading edge- and a trailing edge- control surfaces activated. It has been used for active flutter control research.

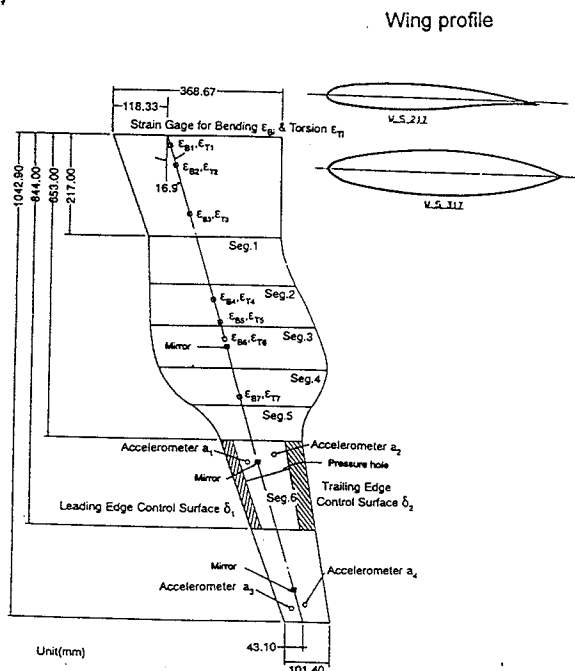


Fig. 2 Aeroelastic model of high aspect ratio wing

Refurbishing items are to provide control surfaces with their activating motors, accelerometers on the wing and a computer for a feedback purpose. Trailing edge- and leading edge- control surfaces were designed to place from 62.6% to 80.9% span position with hinge lines at 73% and 15% chord position, respectively. Since the volume of the geared motors of the necessary torque are too large to be

accommodated within the original cross section of the wing, it was decided to modify the section of the mid wing from original supercritical wing to symmetrical airfoil. To minimize the increase of rigidity, this portion are divided into five parts, made by FRP, and each section is attached to a spar by screws along the elastic axis.

In the present paper, the leading edge control surface is used as a source of excitation and the wing response is represented by an acceleration measured by the sensor at the inward leading edge position (a_1).

Flutter Stopper

2m by 2m section transonic wind tunnel at NAL has a removable test section cart which installs a special device of flutter stopper. A device forms a part of the wind tunnel floor and has a triangular form. When it is protruded into the flow, the dynamic pressure at the test section drops suddenly by as much as 30% and the flutter is stopped. This device is indispensable in executing a wind tunnel flutter test to get an actual flutter boundary. To date the model has experienced as much as 159 times of flutter without any serious damage. It enables to conduct such a wind tunnel test as in the present research because it's necessary to get a lots of hard points of flutter.

Nominal Flutter as a Subcritical Hopf Bifurcation

The previous wind tunnel flutter tests confirmed typical nonlinear characteristics of the transonic flutter such as a transonic dip phenomena and LCO.^(11,12) To get the flutter boundary, the wind tunnel total pressure is set first and then Mach number is increased to a prescribed value. Then keeping the Mach number constant, we increase the tunnel pressure gradually until the wing get flutter. The flutter stopper is activated then to stop the flutter and protect the model.

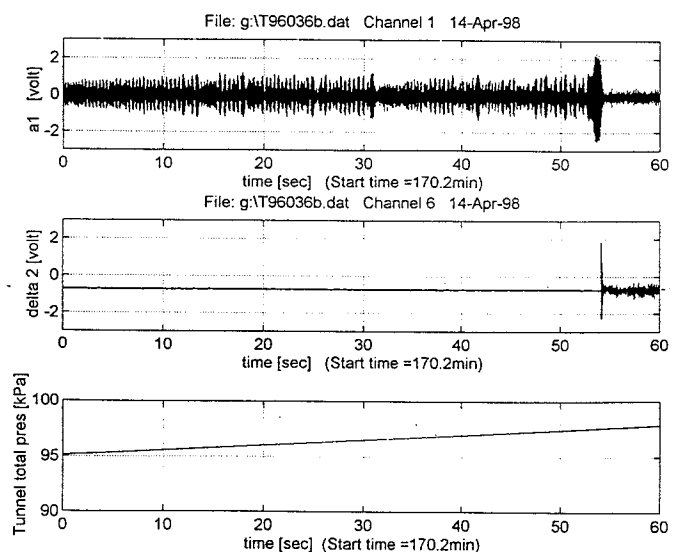


Fig. 3 Time history during increasing total pressure going to nominal flutter.

Figure 3 shows a time chart for 60 seconds of the wind tunnel test to get flutter. Mach number is 0.8. Top chart is a wing response by an acceleration a_1 , bottom is the trend of tunnel total pressure increase. The middle is a trailing edge control surface movement which shows successful recovering from flutter. Chart shows that the tunnel pressure is increasing gradually until flutter occurs. It can be seen that the flutter occurred suddenly as a large amplitude LCO (LC- II). Taking a dynamic pressure as a bifurcation parameter, this phenomena can be more better explained by subcritical Hopf bifurcation than supercritical one. We call this flutter as a nominal flutter since we didn't apply any intentional excitation. We therefore decided to conduct the wind tunnel test to make clear whether it is possible to get flutter even at lower dynamic pressure than nominal value by some kind of excitation.

Qualitative Bifurcation Characteristics

Because LCO is a nonlinear phenomena, the occurrence of LCO may depend on its initial condition. In this respect the wind tunnel turbulence may have effected the dynamic pressure where LCO started to occur. The wind tunnel tests were therefore planned and executed in 1996 to investigate the effect of excitation on the occurrence of LCO. In what follows, Mach number is confined to 0.8.

LCO Induced by LE Excitation

At this first wind tunnel test a limited number of trials were carried out by changing the amplitude of leading edge oscillation at subcritical dynamic pressure. The main objective of this test is to find out whether it is at all possible to get the wing into LCO by excitation at lower dynamic pressure than the nominal pressure and to know what is the lowest dynamic pressure able to get LCO.

In the test a leading edge control surface was used as a source of disturbance by oscillating sinusoidally. The sequence of the oscillating frequency change contains two parts: the frequency is first increased continuously from 10Hz to 30Hz passing through around 20Hz which is near LCO frequency, followed by the second frequency sweep from 10Hz to 20Hz and stopped there. Wind tunnel test conditions are as follows: Mach number $M = 0.8$, wing incidence $\alpha = -0.2$ deg and the offset angle of a leading edge flap $\delta_1 = -2$ deg (setting nose down position).

The test results are that even below the nominal flutter dynamic pressure of 27.6 kPa it is really possible to get a large amplitude LCO (LC- II) if the magnitude of oscillation exceeds a certain level. The wing in equilibrium state were able to jump up to LC- II by leading edge excitation until the dynamic pressure was reduced to 23.8kPa. It was a new finding and

another evidence that our transonic flutter can be explained by subcritical Hopf bifurcation.

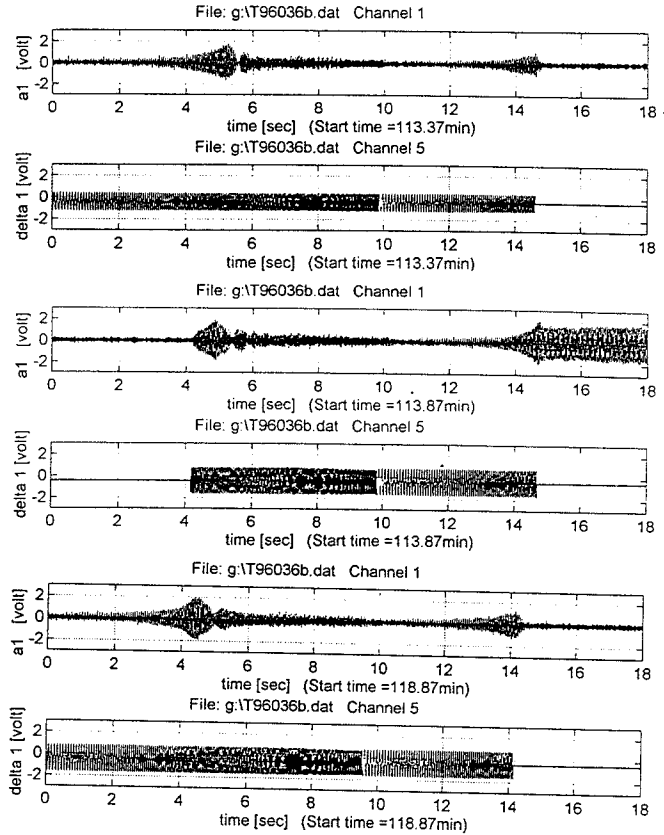


Fig. 4 Wing response due to leading edge excitation

Figure 4 shows three typical responses around a minimum dynamic pressure. At dynamic pressure $P_d=23.8$ kPa and leading edge excitation amplitude of 3 deg, LCO is finally excited as shown in Fig. 4(b). When the frequency was increased from 10 Hz to 30 Hz continuously, LCO once started to occur was suppressed, however, when the frequency was stopped at

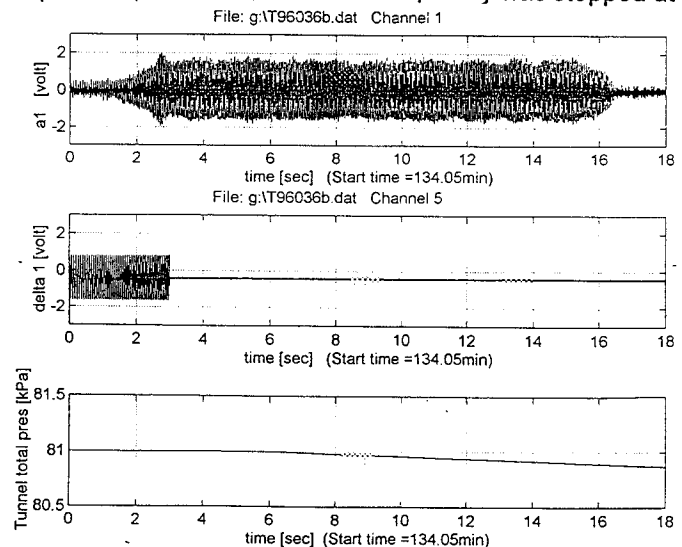


Fig. 5 Quasi-steady decrease of the dynamic pressure at the saddle node bifurcation of LC- II

20 Hz, LCO sustained. The other two time charts are the cases when LCO was not occurred, due to insufficient amplitude of 2 deg in Fig. 4(a) and due to lower dynamic pressure of 23.5 kPa in Fig. 4(c).

Saddle-Node Bifurcation

When we tried to decrease the tunnel pressure during flutter at the minimum pressure, we obtained a time response as shown in Fig. 5. It shows a time history for 18 seconds in which are shown, from top to the bottom, the wing response in acceleration, excitation deflection of a leading edge surface, and a wind tunnel total pressure. It is shown that when the tunnel pressure is decreased a little bit from 81 kPa, the minimum pressure for LCO, to around 80.9 kPa, the flutter suddenly stabilized. This phenomena can be explained as a saddle node bifurcation.

Qualitative Bifurcation Diagram

These several bifurcation can be summarized in a single qualitative bifurcation diagram as shown in Fig. 6.^(13,14) In the figure, dynamic pressure Pd is taken as a control parameter and the angle of attack of the wing, 'alpha', is employed as representing the wing response. The unstable limit cycle is connected to LC-II at a saddle-node bifurcation point. The unstable limit cycle works as a separatrix which separates the attraction basin of the two different solutions. If the wind tunnel noise level or any other disturbance such as a leading edge excitation is enough big to force the system to the other side of the separatrix then flutter of LC-II happens.

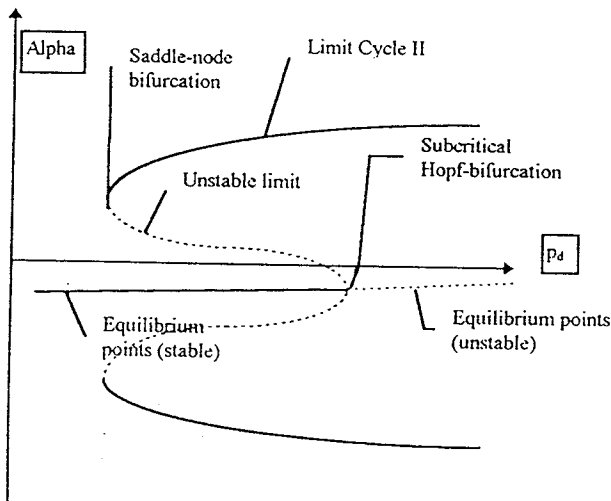


Fig. 6 Qualitative structure of bifurcation diagram

Small Amplitude LCO by Control Disengaged

A more complex dynamics appeared around nominal dynamic pressure accompanied with active control of flutter using a trailing edge control surface. When control was switched off at $p_d=28.3\text{kPa}$, a little bit above the nominal flutter dynamic pressure of

$p_d=27.6\text{kPa}$, a small amplitude LC- I appeared. LC- I disappeared as in a supercritical Hopf bifurcation way such as shown in Fig. 7 where the dynamic pressure was gradually decreased lower than the nominal value. It should be noted that this phenomena does not always happen and its reason is still open.⁽¹³⁾ The supercritical Hopf bifurcation cannot exist with the subcritical Hopf bifurcation at the same time, one possibility is that wing incidence change could lead such a change between the former and the latter. If the supercritical Hopf bifurcation is included around the nominal flutter dynamic pressure range, bifurcation diagram may take the form of Fig. 8.^(13,14)

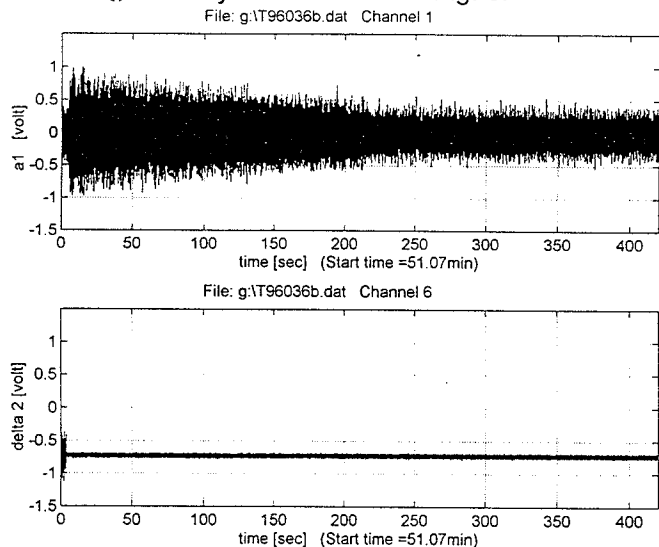


Fig. 7 Supercritical Hopf bifurcation as the dynamic pressure decreasing

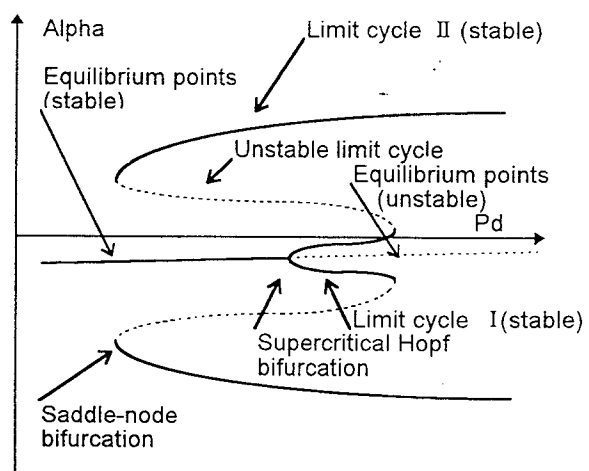


Fig. 8 Bifurcation diagram including supercritical Hopf bifurcation

Follow-on Test of L.E. Excitation

Test procedure and the results

Intending to gain an insight into the bifurcation characteristics for transonic LCO of the wing quantita-

tively, the follow-on tests were planned and executed. The test was conducted to determine the LCO (LC- II) boundary in terms of amplitude of a leading edge excitation at different dynamic pressure. Test conditions are the same as before except the wing incidence of $\alpha = +0.75\text{deg}$. This time oscillation frequency of the leading edge control surface was kept constant at the LCO frequency of 21.5Hz. Test was carried out as follows: first apply the leading edge oscillation and observe whether the wing gets into LCO or not. If wing state can be seen to reach at steady state, LCO or equilibrium, stop excitation. The final step size of the amplitude at the stability boundary were made finer as 0.125deg. Nominal flutter dynamic pressure at this test was a little bit changed to 27.9kPa, mainly due to the change of wing incidence from $\alpha = -0.2\text{deg}$ to $+0.75\text{deg}$, and partly due to the work done for maintenance of the actuating mechanism inside the wing.

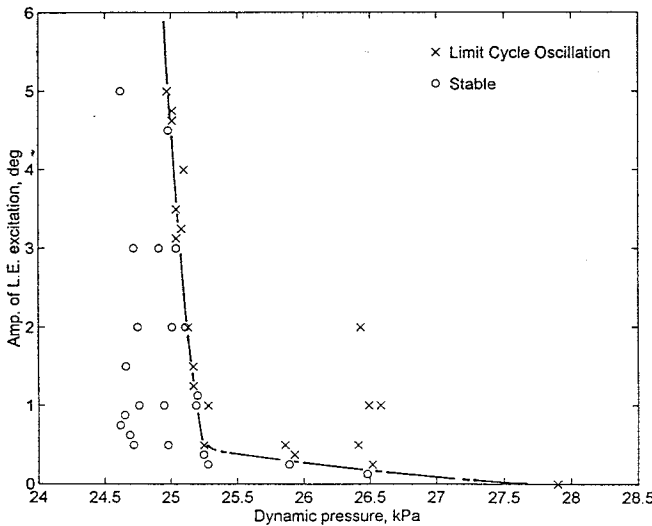
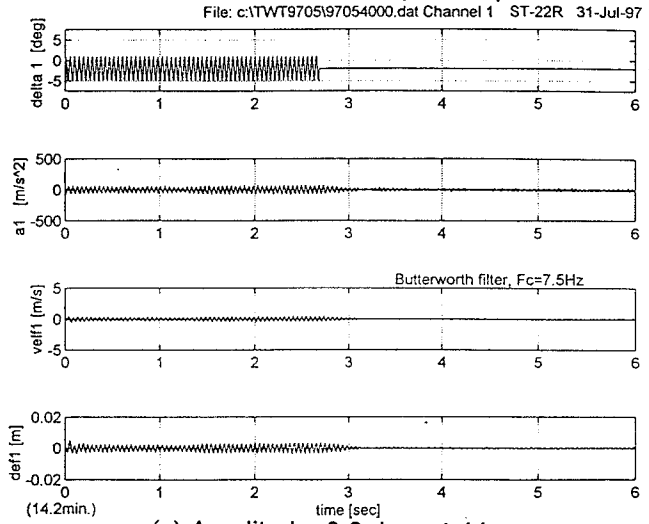


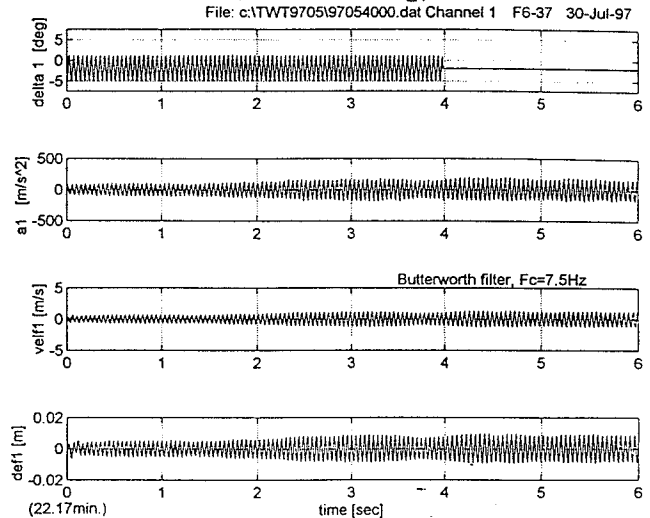
Fig. 9 LCO boundary caused by leading edge excitation

The test results are shown in Fig. 9 which shows stable or LCO for each test point in flap amplitude and dynamic pressure map. Stability boundary between stable- and LCO- points are delineated in the figure; if the excitation amplitude is below the boundary, response of the wing was damped out, but if above, excitation jumped the wing into LCO. Fig. 10 shows these situation by two adjacent test cases, above and below the boundary, at dynamic pressure $Pd=25.04\text{kPa}$ as an example. In these two figures, first channel is the flap deflection and the second channel is the acceleration obtained in the tests. In Fig. 10 (a) even when a leading edge flap excited the wing with 3.0deg amplitude, LCO is not excited, while as in Fig. 10 (b), only 0.125deg higher amplitude excitation

can put the wing into LCO and it continues to oscillate after removal of excitation. The boundary is changed abruptly at around 25.25kPa and the system is globally in equilibrium below 25kPa dynamic pressure.



(a) Amplitude=3.0 deg, stable



(b) Amplitude=3.125 deg, LCO

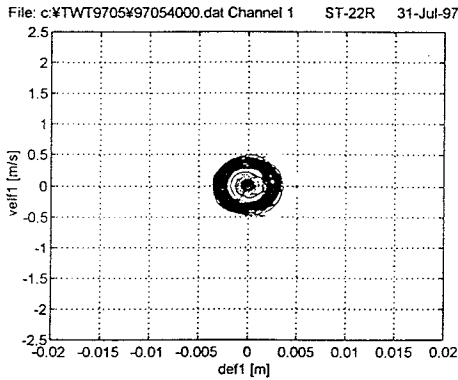
Fig. 10 Wing response due to leading edge excitation ($Pd=25.04\text{ kPa}$)

Phase Diagram and Quantitative Bifurcation Diagram

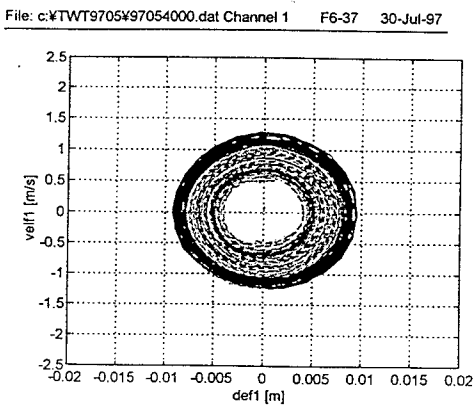
The test data are processed to depict phase diagram. The acceleration signal is numerically integrated twice to get velocity and deflection. In Fig. 10 velocity and deflection obtained by numerical integration of the second channel of acceleration are shown at third and fourth channel. From these data phase diagram can be depicted as shown in Fig. 11 where the response of 3.0deg excitation goes down to origin as in Fig. 11 (a), while the response of 3.125deg goes diverging to LCO as in Fig. 11 (b).

Combining these two phase diagram we can identify the boundary which separates the branches going up to LCO and going down to equilibrium. We can define this boundary as an unstable limit cycle or

separatrix at this particular dynamic pressure. Processing the other four pairs of data at different dynamic pressure in Fig. 9, we can obtain unstable limit cycle data and can plot them in the bifurcation diagram as 'X' mark in Fig.12. Figure 12 is a quantitative expression of a bifurcation diagram which includes a subcritical Hopf bifurcation, a saddle-node bifurcation, a large amplitude LCO, and a stable equilibrium along with an unstable limit cycle.



(a) Stable



(b) LCO

Fig. 11 Phase diagram

Discussion on Math Modeling

Now that the various characteristics of transonic LCO of a high aspect ratio wing model can be expressed by a single quantitative bifurcation diagram: a subcritical Hopf bifurcation at the nominal dynamic pressure, a saddle node bifurcation at the lowest dynamic pressure, and an unstable limit cycle, we can propose a mathematical model which can express these nonlinear phenomena. Here we apply a phenomenological approach, rather than theoretical or computational approach, to obtain empirical math model in a similar but different way as Dowell *et al*⁽¹⁵⁾ proposed for modeling nonlinear oscillator of bluff body aeroelasticity.

For constructing the mathematical model, the following test results should be taken into account:

- (1) At smallest dynamic pressure of LCO, LCO behaves as a saddle-node bifurcation and at the nominal dynamic pressure LCO changes as subcritical Hopf bifurcation.
- (2) Phase diagram of LCO is almost circle and LCO can be assumed as a simple harmonic oscillation.
- (3) The mode of LCO of this wing is almost a single-degree-of-freedom. An oscillating pattern of an outer wing, presented by a quadrilateral of four points where the accelerometers are implemented shows that the outer wing is oscillating as "wash-out" way. Wash-out tendency and a single degree-of-freedom mode at the transonic dip is coincident with the explanation given by Isogai who numerically explored this tendency.⁽¹⁶⁾

Empirical Math Model of Single DOF

Single-degree-of-freedom nature of the present LCO can simplify a model equation. Starting from the similar mathematical model for the system in LCO condition as Cunningham⁽¹⁾, a proposed mathematical model can be expressed as,

$$M\ddot{q} + 2M\zeta\omega_0\dot{q} + M\omega_0^2q = f_a(q) \quad (1)$$

where M, ω_0, ζ , are the generalized mass, LCO frequency, and damping, respectively, q is a generalized coordinate representing the wing LCO response which is in this case a deflection of the wing to the direction of the accelerometer a_1 . $f_a(q)$ is a nonlinear aerodynamic force which drives the wing into limit cycle flutter.

Since bifurcation characteristics is of subcritical type, $f_a(q)$ should have the destabilizing nonlinear term $q^2\dot{q}$ with higher order nonlinear term like $q^4\dot{q}$ to damp the large amplitude oscillation⁽¹⁰⁾ besides a linear stabilizing term. Therefore $f_a(q)$ may have the following structure:

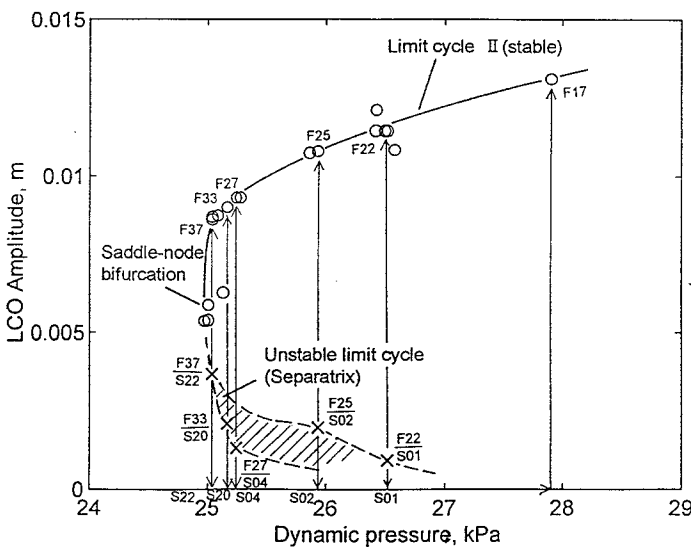


Fig. 12 Quantitative subcritical Hopf bifurcation diagram

$$f_a(q) = P_d S (a + bq^2 - cq^4) \dot{q} / U \quad (2)$$

where $P_d = (1/2)\rho U^2$ is a dynamic pressure. In eq. (2), the second and third term together may present the loss of aerodynamic efficiency of the first term due to some sort of flow separation caused by a shock or at the middle part of the wing. Substituting eq.(2) to eq.(1), we get

$$\ddot{q} + \left(2\zeta - a \frac{P_d f S}{MU\omega_0} \frac{P_d}{P_d f} \right) \omega_0 \dot{q} - \frac{P_d f S}{MU\omega_0} \frac{P_d}{P_d f} (bq^2 - cq^4) \omega_0 \dot{q} + \omega_0^2 q = 0 \quad (3)$$

where P_{df} is a nominal flutter dynamic pressure to be featured subcritical Hopf bifurcation. With the unit of time and length such as,

$$\text{Time: } \frac{1}{\omega_0}$$

$$\text{Length: } \frac{1}{\sqrt{bv}}; \quad v = \frac{P_{df} S}{MU\omega_0}$$

we define the non-dimensional time τ and deflection \tilde{q} as,

$$\tau = \omega_0 t$$

$$\tilde{q} = \sqrt{bv} q$$

Equation (3) is non-dimensionalized with these variables as,

$$\tilde{q}'' - \left\{ a v \left(\frac{P_d}{P_{df}} - 1 \right) + \frac{P_d}{P_{df}} (\tilde{q}^2 - \mu_3 \tilde{q}^4) \right\} \tilde{q}' + \tilde{q} = 0 \quad (4a)$$

where $()'' = \frac{d^2()}{d\tau^2}$, $()' = \frac{d()}{d\tau}$, and $\mu_3 = \frac{c}{b^2 v}$.

Equation (4a) is further simplified introducing additional parameters such as

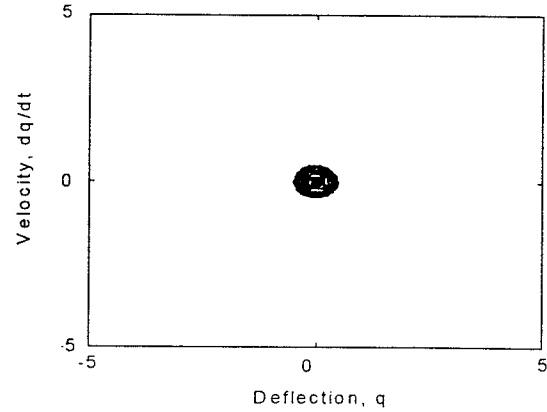
$$\mu_1 = \frac{av}{P_{df}} p_d = \frac{aS}{MU\omega_0} P_d, \quad \mu_f = av = \frac{aS}{MU\omega_0} P_{df}$$

, and $\mu_3 = \frac{c}{b^2 v}$ along with an artificial parameter

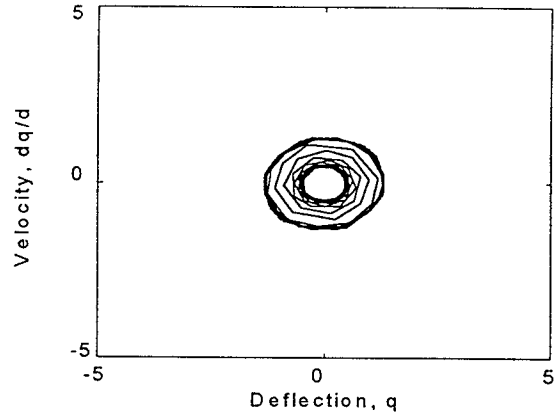
$$\mu_2 = 1.$$

$$\tilde{q}'' - \left\{ (\mu_1 - \mu_f) + \mu_2 \frac{\mu_1}{\mu_f} \tilde{q}^2 - \mu_3 \frac{\mu_1}{\mu_f} \tilde{q}^4 \right\} \tilde{q}' + \tilde{q} = 0 \quad (4b)$$

where only μ_1 is a function of dynamic pressure P_d .



(a) Initial condition: $(\tilde{q}_0, \tilde{q}'_0) = (0.49, 0)$



(a) Initial condition: $(\tilde{q}_0, \tilde{q}'_0) = (0.50, 0)$

Fig. 13 Phase diagram of numerical simulation of eq. (4b). $\mu_1 = 0.95$

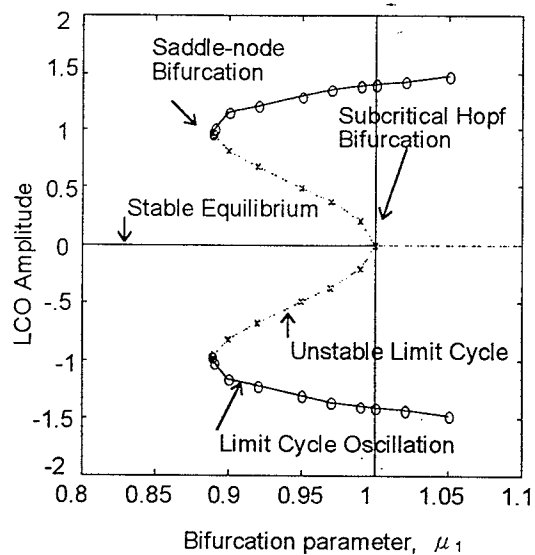


Fig. 14 Empirical mathematical model for transonic LCO flutter

Numerical simulation of the equation

The nonlinear equation (4b) can be numerically simulated using Matlab/Simulink software. Intending to place the saddle-node at around 10% lower point to subcritical Hopf bifurcation, the values of the parameters in eq. (4b), $\mu_2 = 1$, $\mu_3 = 1$, along with $\mu_f = 1.0$ are chosen and the equation was analyzed numerically with μ_1 as a control parameter. Since the equation is nonlinear, the solution depends on initial conditions. The dependency of the initial conditions determine the boundary, i.e., unstable limit cycle, which separates the solution going to LCO and the one going to a stable equilibrium. For example at $\mu_1 = 0.95$, the initial condition, $(\tilde{q}_0, \tilde{q}_0') = (0.49, 0)$, yields the stable solution, while the initial condition, $(\tilde{q}_0, \tilde{q}_0') = (0.50, 0)$, yields the LCO solution as shown in Fig. 13 as a phase diagram. The result of the simulation can be summarized in Fig. 14 where a stable equilibrium ends up at a subcritical Hopf bifurcation, connected with a saddle-node bifurcation to a large amplitude LCO. These fundamental structures well represent the quantitative bifurcation of Fig. 12.

Concluding Remarks

Several nonlinear phenomena were found during series of wind tunnel tests in the transonic region for a high aspect ratio wing model: at nominal dynamic pressure without any intentional excitation, flutter emerged as a large amplitude limit cycle oscillation in a subcritical Hopf bifurcation way. Using a leading edge surface excitation, LCO appeared until as lower as 10% below the nominal flutter dynamic pressure. At a smallest dynamic pressure, LCO jumped down to a stable equilibrium via a saddle-node bifurcation. Between these dynamic pressure, unstable limit cycle which connects the saddle-node bifurcation and subcritical Hopf bifurcation can be identified as a boundary separating LCO and a stable equilibrium region. Quantitative bifurcation diagram was thus obtained by the test and an empirical math model of single degree-of-freedom is proposed. Another possibility of supercritical Hopf bifurcation still exists since a small amplitude LCO appeared just above a nominal flutter dynamic pressure when an active flutter control was turned off and disappeared continuously to a stable equilibrium as the dynamic pressure was decreased.

References

1. Cunningham, A. M., Jr., "Practical Problem: Air-planes,"

- Chapter 3, *Unsteady Transonic Aerodynamics*, Nixon, D., ed., Progress in Astronautics and Aeronautics, Vol. 120, AIAA, 1989, pp. 75-132.
2. Dowell, E. H., "Nonlinear Aeroelasticity," *Flight-Vehicle Materials, Structures and Dynamics*, Vol. 5. Part II, Chapter 4, ASME, 1993, pp. 213 - 239.
3. Ueda, T. and Dowell, E. H., "Flutter Analysis Using Non-linear Aerodynamic Forces," *J. Aircraft*, Vol. 21, No. 2, Feb. 1984, pp. 101-109.
4. Bendiksen, O. O. and Hwang, G-Y., "Nonlinear Flutter Calculations for Transonic Wings," Proceedings of CEAS International Forum on Aeroelasticity and Structural Dynamics 1997, Vol. II, Rome, 1997, pp. 105-114.
5. Kheirandish, H., Beppu, G., and Nakamichi, J., "Flutter Simulation by Navier-Stokes Equations," Proceedings of the 34th Aircraft Symposium, FSASS, 1996, pp.545-548.
6. Meijer, J. J. and Cunningham, A. M., Jr., "Online and Applications of a Semi-Empirical Method for Predicting Transonic Limit Cycle Oscillation Characteristics of Fighter Aircraft," Paper No. 75, Proceedings of Int'l. Forum on Aeroelasticity and Structural Dynamics, 1995, pp. 75.1 - 75.19.
7. Timmermann, H., and Tichy, L., "Application of the Hilbert Transform to Flight Vibration Testing," Paper No. 78, Proceedings of Int'l. Forum on Aeroelasticity and Structural Dynamics, 1995, pp.78.1 - 78.13.
8. Schewe, G. and Deyhle, H., "Experiments on Transonic Flutter of a Two-Dimensional Supercritical Wing with Emphasis on the Non-Linear Effects," Proceedings of the Royal Aeronautical Society Conference on "UNSTEADY AERODYNAMICS", 1996.
9. Strogatz, S. H., *Nonlinear Dynamics and Chaos*, Addison-Wesley Publishing Co., 1994.
10. Bergé, P., Pomeau, Y., and Vidal, C., *Order within Chaos*, John Wiley & Sons, 1984.
11. Matsushita, H., Hashidate, M., Saitoh, K., Ando, Y., Fujii, K., Suzuki, K. and Baldelli, D. H., "Transonic Flutter Control of a High Aspect Ratio Wing: Mathematical Modeling, Control Law Design and Wind Tunnel Tests," Proceedings of 19th ICAS, Anaheim, 1994, pp. 2070-2079.
12. Saitoh, K., Hashidate, M., Matsushita, H., and Kikuchi, T., "Elastic Deflection Effects on Transonic Aerodynamics of a Flutter Wing Model with Control Surfaces," 1st AIAA Aircraft Engineering, Technology, and Operations Congress, Los Angeles, AIAA 95-3926, 1995.
13. Gránásy, P., Matsushita, H., and Saitoh, K., "Nonlinear Aeroelastic Phenomena at Transonic Region," Proceedings of CEAS International Forum on Aeroelasticity and Structural Dynamics 1997, Vol. III, Rome, 1997, pp. 379-385.
14. Gránásy, P., Matsushita, H., and Saitoh, K., "Nonlinear Analysis of Transonic Flutter," The proceedings of the 10th International Sessions in Aircraft Symposium, JSASS, 1996, PP. 66-69.
15. Dowell, E. H. and Ilganov, M., *Studies in Nonlinear Aeroelasticity*, Springer-Verlag, 1988.
16. Isogai, K., "On the Transonic-Dip Mechanism of Flutter of a Sweptback Wing," *AIAA Journal*, Vol. 17, No. 7, pp. 793-795.